Development and Testing of a Solar Flux Heating Freeze Recovery System for Molten Salt Parabolic Troughs

Luca Imponenti[1, a)], Juan Carlos Herruzo[2], Ryan Shininger[1], Hank Price[1] and Juan Valverde[2, 3, b)]

[1]*Solar Dynamics LLC, 1105 W 11th Ct, Broomfield, CO, 80020, USA*
[2]*Virtualmech, Parque Empresarial Torneo c/ Arquitectura 1, Torre 6, Planta 10ª, 41015, Seville, Spain*
[3]*Dept. of Applied Mathematics II. University of Seville. Camino de los Descubrimientos s/n, 41092, Seville, Spain*

[a)]luca.imponenti@solardynllc.com
[b)]j.valverde@virtualmech.com

Abstract. A major obstacle preventing commercialization of molten salt parabolic trough plants is freeze protection and recovery of the solar field. One of the most common nitrate salt compositions under consideration allows for solar field outlet temperatures up to 565°C and begins solidifying above 240°C. Using molten salt directly in the solar field can significantly reduce thermal energy storage costs and the higher temperature compared to oil heat transfer fluids can power a more efficient power cycle, but the very high freezing point is cause for concern. This work builds on a previous modeling effort investigating different methods for melting Solar Salt frozen in the solar field, which suggested the viability of a novel solar heating method to lower costs of the freeze protection system. In this work higher fidelity models are developed to better investigate the melting process with a more detailed 3D geometry which includes the insulated bellows. The thermal-fluid model of the melting process is updated to include temperature dependent density and data for solid phase properties. In addition, a finite element model is developed to resolve thermal stresses at the point with highest thermal gradients. Results with the new model confirm the viability of using controllable solar flux heating to thaw salt frozen in the solar field without damaging the receiver; however, the presence of non-illuminated sections significantly slows down the melting process. Solar heating simulations with pauses off-sun of 120 and 60 s require 18.5 and 11.9 h to melt salt from a night-time temperature of 10°C with 1000 W m^2 DNI, which results in maximum thermal stresses of 48.2 and 53.5 MPa, respectively. Adding 150 W m^{-1} to the solar heating simulation with a 60 s pause off-sun decreases both the melt time and thermal stresses due to the more uniform heating, suggesting a combined heating method may be the best option.

INTRODUCTION

Parabolic trough collectors are among the most mature concentrated solar power (CSP) technologies, with many operational plants around the world. Coupling CSP and thermal energy storage (TES) can yield greater penetration of renewables onto the grid by providing dispatchable solar energy during times of high demand[1]. The next generation of parabolic trough systems under consideration uses molten salt as both the TES media and heat transfer fluid (HTF) in the solar field, which could significantly reduce the cost of TES compared to plants that use biphenol/diphenol oxide HTFs. Commonly used TES media include the nitrate salt mixtures such as Solar Salt and HITEC. These mixtures have high freezing points above 100°C, thus the prevention and recovery of salt freezing in the solar field must be designed for when using molten salt as the HTF. Considering a worst-case scenario, the plant must be designed to recover from a complete freeze event. The current approach is to use heat tracing in the header piping and impedance heating in the collector receiver tubes[2]; while this is an effective solution the impedance heating system can be a significant portion of the solar field costs. Previous 2D modeling studies investigating the use of low-intensity mirror flux profiles to replace or supplement impedance heating systems for freeze recovery in molten salt parabolic troughs indicated this heating method showed potential to be a more cost-effective solution. In order to attenuate the heat input from the mirrors for this application a track-trough method for cycling the mirrors on and off-focus was introduced

and investigated with a preliminary model[3]. This work builds on previous modeling studies with a detailed 3D representation of the HCEs, and more complex physics through updated thermophysical property functions. Results from this modeling study will guide experimental work to test the solar flux heating concept on-sun with a single trough module as part of the DOE project: Simplified Melting And Rotation-joint Technology for Molten Salt Troughs (SMART).

MODEL DESCRIPTIONS

To resolve thermal stresses throughout the melting process thermal-fluid and thermal-mechanical models are developed in ANSYS Fluent and Mechanical [4]. The thermal-fluid model considers a typical HCE with 90 mm diameter and 4 mm wall thickness. There are symmetry conditions at the axial center of the HCEs and bellows. The detailed 3D geometry and mesh is shown in **FIGURE 1**, with the non-illuminated section clearly visible on the left side. The full structure including the glass envelope is modeled. The detailed geometry allows for realistic thermal and structural boundary conditions to accurately represent the real-world thawing process. Temperature profiles from the thermal fluid model are input to the mechanical model to resolve thermal stresses resulting from the melting process. The von Mises stresses determined from the model are compared to ASME Section II allowable values to assess the viability of different heating methods.

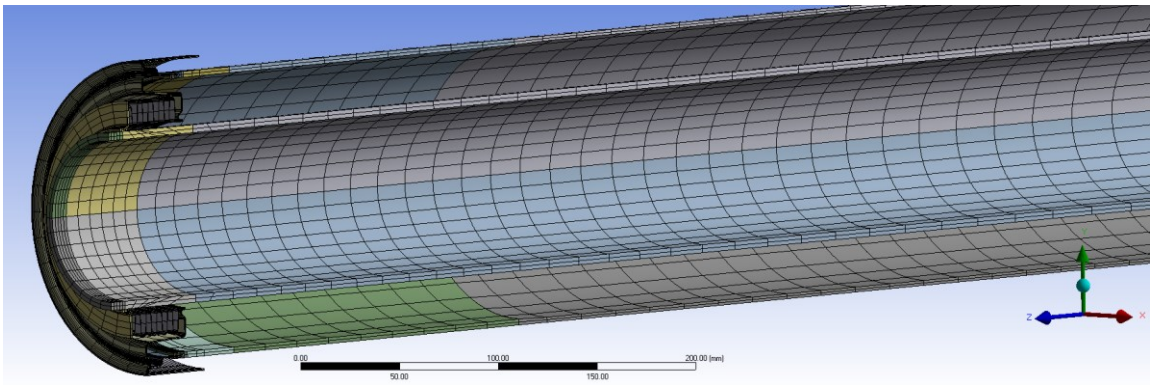

FIGURE 1. Illustration of detailed HCE geometry and mesh. Although axial cross-section is shown for clarity, the full circumference of the HCE is modeled.

Thermal-Fluid Model

The thermal fluid model solves the transient, conjugate heat transfer problem between two fluid domains (salt in HCE, vacuum in glass envelope) and the HCE structure. Modeling the glass envelope gives the model flexibility in terms of heat loss boundary conditions. Solar Salt is considered for all simulations. The general fluid model description and receiver tube material properties are detailed in a previous publication[3]. To numerically model the melting process an enthalpy-porosity technique is used [5], i.e., the liquid fraction of molten salt in each cell is tracked via the liquid fraction, β. For each cell, β is calculated based on the cell temperature and salt phase diagram. $\beta = 0$ corresponds to solid salt, $\beta = 1$ is molten salt. Cells with $0 < \beta < 1$ are referred to as the mushy zone and modeled as a porous medium. The momentum equation for the enthalpy-porosity method is written in Eq. 1.

$$\frac{\partial}{\partial t}(\rho\vec{v}) + \nabla\cdot(\rho\vec{v}\vec{v}) = -\nabla p + \nabla\cdot\left[\mu\left(\nabla\vec{v} + \nabla\vec{v}^{T} - \frac{2}{3}\nabla\cdot\vec{v}I\right)\right] + \rho\vec{g} + \frac{(1-\beta)^2}{(\beta^3+\varepsilon)}A_{\text{mush}}\vec{v} \quad (1)$$

where A_{mush} and ε are modeling parameters set to 10^5 and 10^{-3}, respectively. The parameter A_{mush} is a damping factor governing the transition of the velocity to zero as it solidifies. This parameter can vary for different fluids and should be determined experimentally, but the selected value works well for many cases[6]. Furthermore, the latent energy associated with the phase transition appears in the salt enthalpy equation as follows,

$$H = h_{\text{ref}} + \int_{T_{\text{ref}}}^{T} c_{\text{p}}\, dT + \beta\Delta h_{\text{f}} \quad (2)$$

where h_{ref} is the reference enthalpy of the fluid at the reference temperature, T_{ref}. The specific heat integral captures the sensible energy required to heat the salt, while the latent energy term is directly proportional to β.

The thermophysical properties of Solar Salt in the new model were updated to capture variations during the melting process, significantly increasing model complexity. Modified properties are plotted in **FIGURE 2**, these include temperature-dependent density to capture buoyant forces, specific heat with additional peak for the solid-solid phase transition, and thermal conductivity updated to include solid phase data[7]. Furthermore Δh_{f} is changed to 115520 J kg^{-1}, since the solid-solid phase transition is accounted for in the specific heat function[8].

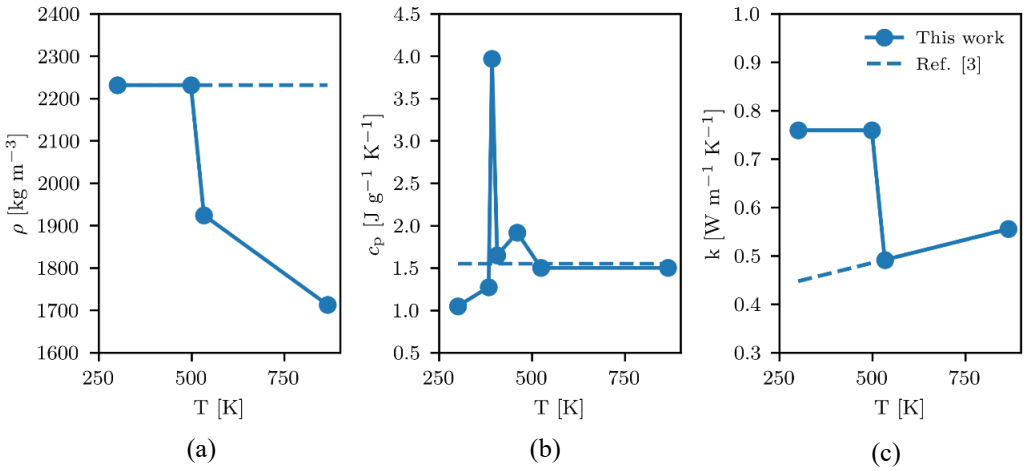

FIGURE 2. Thermophysical properties of Solar Salt updated to include variations during phase change and solid phase properties as measured in Iverson et al. 2012. (a) Density[9], (b) specific heat[7], and (c) thermal conductivity[7] used in thermal-fluid model. The specific heat curve includes the solid-solid phase transition occurring around 120°C[8].

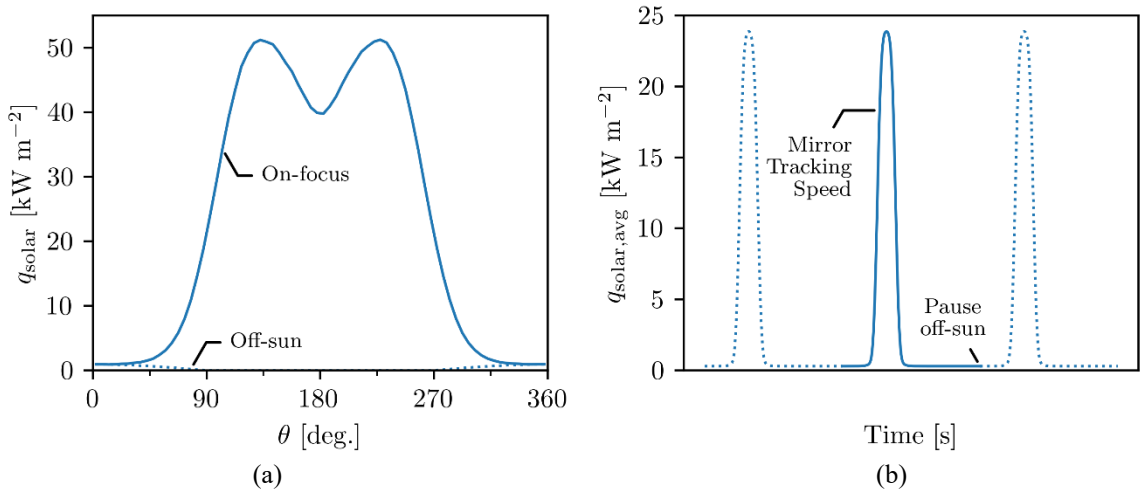

FIGURE 3. (a) Solar flux profile around the illuminated section of the HCE for different mirror positions, and (b) transient, spatially averaged heat flux input to HCE by rotating the mirrors between off-sun and on-focus positions

The boundary conditions include symmetry conditions at the center of the HCEs and bellows, and a heat flux condition on the outer absorber tube wall. The heat flux condition may include a Joule heating component modeled as constant heat flux, and/or a solar heating component. To safely use concentrated solar heat from the parabolic mirrors a track-trough method is used[3], wherein the mirrors are cycled between on-focus and off-sun positions as shown in **FIGURE 3**. Heat losses are inherently captured by modeling the vacuum space in the glass envelope. For the fluid domains there are no-slip conditions at the inner absorber tube surface, as well as the outer absorber surface and inner glass envelope wall.

Thermal-Mechanical Model

A finite element model is used to analyzed results from the thermal-fluid model and resolve stresses in the glass envelope and absorber tube. To accurately model the constraints of a long string of HCEs, such as a full-scale collector, the geometry used for the thermal fluid simulation is not sufficient. For the mechanical model the temperature profile of interest is projected across two HCEs, taking advantage of the symmetry conditions at the center of the HCE and bellows. A static structural analysis is performed on the two HCE string using the temperature profile with the largest thermal gradients observed during the melting process.

RESULTS & DISCUSSION

When comparing results from simulations with different heating method it is useful to consider the time and space averaged heat input, $\bar{q}$, written in Eq. 3. $\bar{q}$ provides a measure of the total heat input to the HCE.

$$\bar{q} = \frac{1}{t_{melt}} \int_0^{t_{melt}} \left(q_{imp} + \frac{R_o}{L} \int_0^L \int_0^{2\pi} q_{solar} \right) \quad (3)$$

All solar heating simulations presented in this document were performed with 1000 W m^{-2} DNI and 0° incidence angle. Results for simulations completed thus far are summarized in **TABLE 1**. For Joule heating a 250 W m^{-1} limit was considered based on previous freeze recovery studies. For solar heating simulations 120 s was selected as the limit from 2D modeling studies[3].

TABLE 1. Summarized results of thermal-fluid model.

Case #	Impedance Heat [W m^{-1}]	t_{off} [W m^{-2}]	$\bar{q}$ [W m^{-1}]	% Impedance Power	t_{melt} [h]	$\sigma_{\text{VM,max}}$ [MPa]
1	250	-	250	100.0	12.0	39.8
2	0	120	254	0.0	18.5	48.2
3	0	60	387	0.0	11.9	53.5
4	150	60	537	28.0	6.75	45.7

Melting Process

The model described in this paper is the most detailed study investigating freeze recovery for an HCE filled with molten salt to date. Compared to previous 2D modeling studies with constant density, the insulated bellows and natural convection heat transfer significantly affect the melt process. The time for the melting process to begin and end from an initial temperature of 10°C is plotted **FIGURE 4**(a). These results indicate a significant difference between impedance and solar heating simulations with similar values of $\bar{q}$, caused by the non-illuminated zone included in the 3D geometry. For simulations with no impedance heating component salt thawed in the illuminated section of the HCE must melt salt in the bellows resulting in significant heat transfer along the length of the HCE; compared to impedance heating simulations with a lower, uniform heat input where heat propagates radially and axial gradients are caused only by differences in heat losses. This phenomenon increases t_{melt} for solar heating compared to similar 2D simulations. This result also demonstrate the significant differences between conduction-dominated heat transfer before the onset of melting and convection once the salt has begun to thaw. The time required for the onset of melting is very similar for both impedance and solar heating simulations with $\bar{q} \approx 250$ W m^{-1}, but the melt process takes significantly longer with solar heating once there is liquid salt in the system to effectively transfer heat to non-illuminated zones. Simulations with a solar heating component appear to follow a linear trend of decreasing melt time as $\bar{q}$ increases, even with an added component of impedance heating. However more data is required to better understand this relationship.

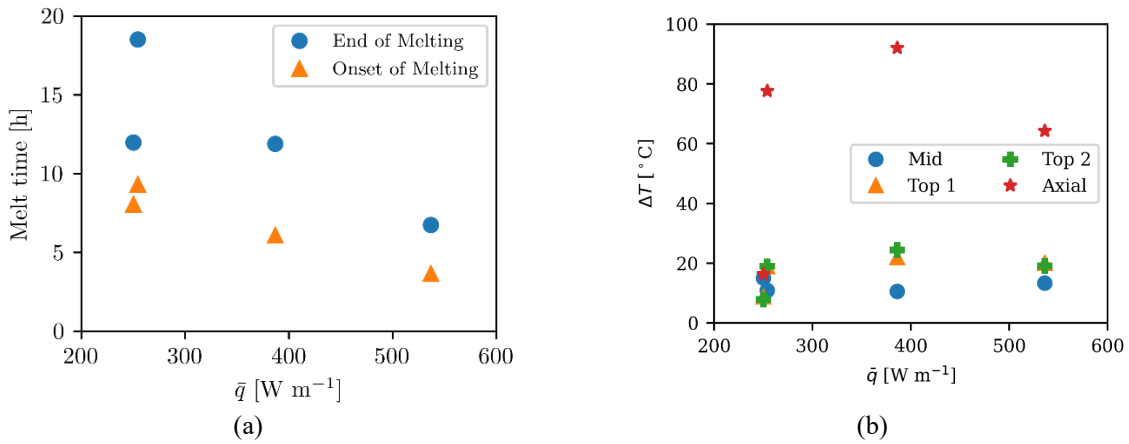

FIGURE 4. (a) Time for onset and end of melting process. (b) Maximum temperature differences across different cross-sections of the HCE during melting: Mid – middle of HCE, Top1 – HCE and bellow interface, Top2 – center of bellows, Axial – considers Mid and Top2 sections.

The temperature differences, ΔT, observed at different sections of the absorber tube are plotted in **FIGURE 4**(b). Simulations with solar heating show significantly higher axial ΔT due to the presence of the non-illuminated bellows; however, the circumferential gradients are maintained below 25°C in all cases. These results demonstrate the benefits of combining impedance and solar heat inputs, since the simulation with largest heat input (Case 4) shows decreased values of ΔT for all except the Mid location (center of the HCE), compared to a case with the same solar heat input but no impedance component (Case 3). Thus, adding a component of impedance heating shows potential to lower thermal gradients while also decreasing the melt time. A representative temperature contour plot for pure solar heating of the HCE is shown in **FIGURE 5**; this plot shows the axial gradient caused by the non-illuminated zone on the left side, and the comparatively small ΔT between the top and bottom of the absorber tube.

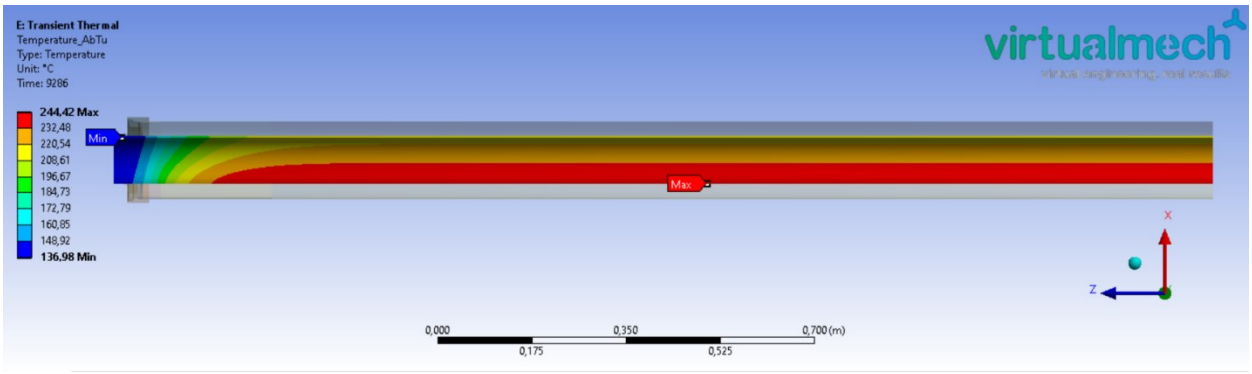

FIGURE 5. Temperature profile through an axial cross-section for a pure solar flux heating simulation, Case 3.

Considerations for Solar Heating

One of the goals for this modelling effort is to assess the viability of solar flux heating for thawing salt frozen in the HCEs. Reducing the scope of the impedance heating system to only the collector interconnects would result in the highest possible cost savings for a novel freeze protection system[3]. Results thus far suggest the method is possible but challenging due to the 10+ hours of perfect weather conditions required, although more aggressive heating profiles are being explored to lower this value the weather dependency will remain a challenge. In addition, the collector interconnects (assumed to be flex hoses in this project) are heated electrically, so great care must be taken to ensure the electrical and solar components of the system heat at a similar rate. However, natural convection greatly enhances heat transfer in the bulk salt, and results indicate that pure solar heating will safely melt salt thawed in non-illuminated zones of the collector. The salt temperature extrema for illuminated and non-illuminated zones during melting from

10°C are plotted in **FIGURE 6**, which shows the onset of convective heat transfer when the salt begins melting. Before the onset of melting the ΔT between the HCE and bellows regions constantly increases with time. After the onset of melting, heat transfer to the non-illuminated zone is greatly enhanced and the temperature begins to equilibrate with the illuminated zone. Although the highest axial gradient occurs just before the melt onset, the worst-case circumferential gradient occurs closer to the end of melting when a large fraction of salt is melted. The higher density solid salt sinks and causes a cold spot near the absorber tube surface, resulting in a circumferential ΔT. Results indicate the time required for solar heating is a significant challenge considering weather constraints. In addition, any HCEs with lost vacuum or completely broken glass will have increased heat losses which will drive axial heat transfer and further slow down the melt process, similar to the bellows. For these reasons the combined impedance and solar heating system is seen as a more robust solution; however, a more detailed cost analysis is required to fully assess the benefits of a combined system and determine if the additional cost savings associated with pure solar heating are worth pursuing.

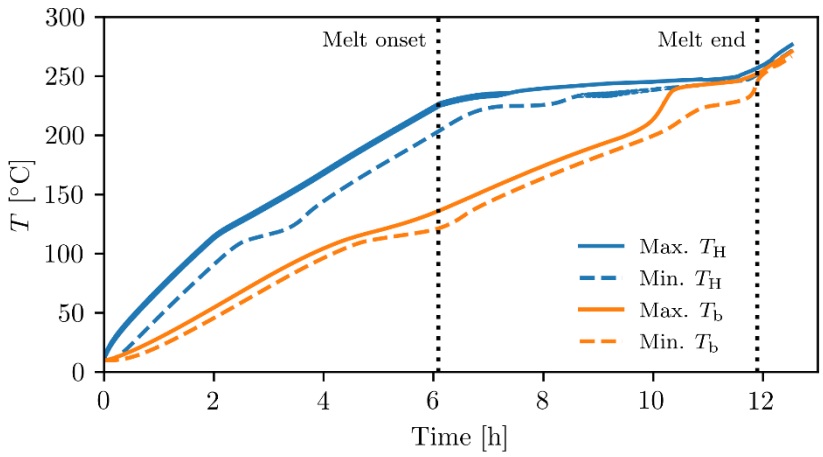

FIGURE 6. Comparison of temperature profiles in the middle of the HCE (subscript H) and the insulated bellows (b) for a pure solar flux heating simulation, Case 3.

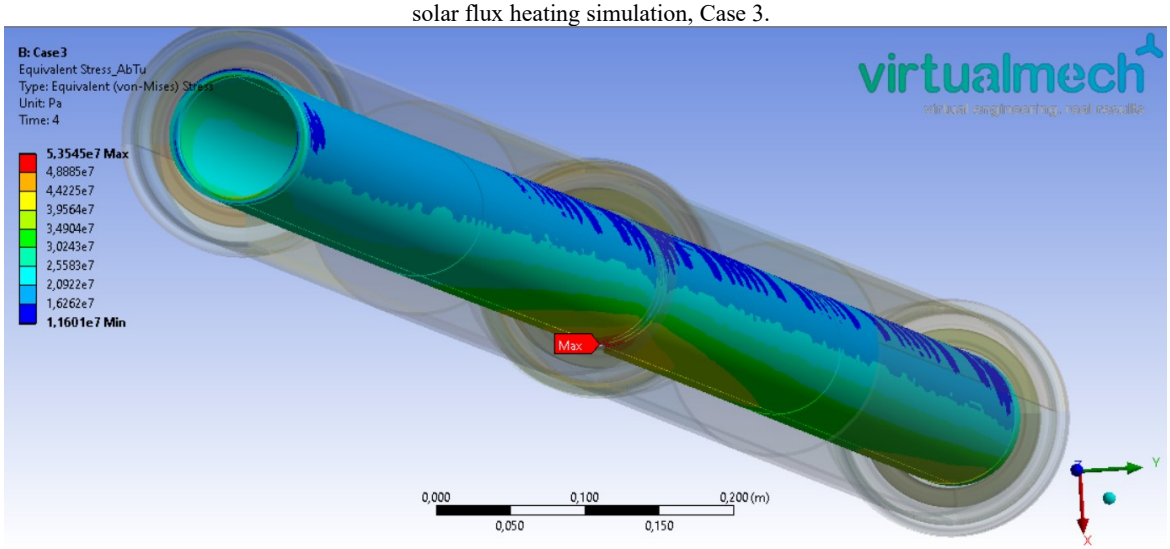

FIGURE 7. Stress contour at time with largest observed thermal gradient for Case 3.

Thermal Stresses

Stresses are calculated in ANSYS Mechanical using temperature data from the time step with the largest thermal gradient observed during the thermal-fluid simulations. All the simulations completed thus far show stresses well below ASME Section II allowable values (129 MPa at 200°C)[10]. The resulting von Mises stress profile for a typical

solar simulation is illustrated in **FIGURE 7**. The high stress point occurs at the welded interconnect in between HCEs, this weak point was consistent between simulations with different heating types. The values in **FIGURE 7** are mainly thermal stresses due to the non-uniform temperature profile generated during melting with an internal pressure of 1 bar in absorber tube. Despite the significantly larger axial gradients present in solar heating simulations compared to impedance heating, circumferential gradients are more important for generating thermal stresses in this geometry. A parametric analysis looking at the internal pressure indicates any additional expansion forces superimposed on the thermal stresses will quickly result in failure. This result suggests the tube will fail if a large volume of salt is constrained such that it expands into the tube.

CONCLUSION

This modeling effort investigated the melting process of Solar Salt in a parabolic trough HCE through thermal-fluid and thermal-mechanical modeling. Results qualitatively support the conclusions from a previous simplified modeling study suggesting the viability of a novel solar flux heating method[3], despite significantly different quantitative results due to the more complex physics and detailed geometry in the updated model. Compared to more common impedance heating systems, solar flux heating provides non-uniform heat using the parabolic mirrors and presents an opportunity for cost savings in the required freeze protection and recovery system. A solar flux heating process with a 60 s pause off-sun will melt Solar Salt frozen to 10°C in 11.9 hours with a maximum von Mises stress of 53.5 MPa. More aggressive solar heat flux profiles are being explored since the stresses are well below allowable stress values. Adding 150 W m^{-1} of impedance heating to the previous solar heating simulation reduces both the melt time and maximum von Mises stress to 6.75 hours and 45.7 MPa, respectively. The more expensive combined heating system appears to be the better technical solution, so a cost analysis will be important to determine the best system.

Future work includes finalizing certain model simulations, building an experimental test setup to validate these model results and prove the solar heating concept on-sun, and a detailed cost analysis. Future model simulations will look to push the HCE to higher stress levels to understand the limitations of this heating method, and match experimental conditions for model validation. Comparing the model to experimental data will allow tuning of the parameter A_{mush}, which has been shown to impact model results and should be fit to experimental data[6]. In addition, a detailed cost analysis will be performed to quantify the economic impact of different levels of solar heating; while a component of electrical heating is inevitable, minimizing this component will lower costs. Together this information should provide a complete picture of the freeze recovery options for molten salt parabolic trough plants, addressing one of the major uncertainties for the commercialization of molten salt parabolic trough plants.

ACKNOWLEDGMENTS

This material is based upon work supported by the U.S. Department of Energy's Office of Energy Efficiency and Renewable Energy (EERE) under the Solar Energy Technologies Office Award Number DE-EE0008140.

REFERENCES

1. P. Denholm and M. Mehos, Enabling Greater Penetration of Solar Power via the Use of CSP with Thermal Energy Storage (2011).
2. D. Kearney, B. Kelly, U. Herrmann, R. Cable, J. Pacheco, R. Mahoney, H. Price, D. Blake, P. Nava, and N. Potrovitza, Energy **29**, 861 (2004).
3. L. Imponenti, R. Shininger, K. Gawlik, H. Price, and G. Zhu, J. Energy Resour. Technol. **142**, (2020).
4. ANSYS Inc., ANSYS Fluent, Release 18.2, Help Syst. (n.d.).
5. V.R. Voller and C. Prakash, Int. J. Heat Mass Transf. **30**, 1709 (1987).
6. M. Fadl and P.C. Eames, Appl. Therm. Eng. **151**, 90 (2019).
7. B.D. Iverson, S.T. Broome, A.M. Kruizenga, and J.G. Cordaro, Sol. Energy **86**, 2897 (2012).
8. R. Benages-Vilau, T. Calvet, M.A. Cuevas-Diarte, and H.A.J. Oonk, Phase Transitions **89**, 1 (2015).
9. A.B. Zavoico, Solar Power Tower Design Basis Document (2001).
10. ASME, BPVC.II.D.M-2017 (2017).